Seismic fragility curves for mid-rise reinforced concrete framed structures with different lateral loads resisting systems

Ghada Mousa Hekal [a], Kamel Kandeel [a,*], Mostafa Morsi El-Shami [b], Ahmed Dawod [a]

[a] *Department of Civil Engineering, Menoufia University, Shebin ElKoum, Menofia, Egypt*
[b] *Department of Construction Engineering, University of Dammam, Dammam 34212, Saudi Arabia*

ABSTRACT

The current study presents lateral load analysis of mid-rise reinforced concrete framed structures with two different lateral load resisting systems; shear walls and rigid marginal beams. The main objective here is to investigate the influence of the location of the system in the structure; i.e. arrangement of shear walls and level of the marginal beam. For that purpose, seismic fragility curves are used as an assessment tool for comparing the seismic performance of the studied structures in different situations. Incremental dynamic analysis was performed under ten ground motions to determine the yielding and collapse capacity of each building. Five performance levels were considered in the analysis. These performance levels are (i) operational, (ii) immediate occupancy, (iii) damage control, (iv) life safety and (v) collapse prevention. Fragility curves were developed for the structural models of the studied structures considering the previously mentioned performance levels. It was observed that arrangement of shear walls on the long direction of the structure has insignificant effects on its performance while interior shear walls provide the best behavior of the structure compared to exterior shear walls only and distributing shear walls internally and externally. The analysis outcomes also indicated that the presence of the rigid marginal beam in the lower storey gives more efficiency regarding to lateral loads resistance in the studied structure.

ARTICLE INFO

1. Introduction

Shear walls and rigid marginal beams are the most common tools used for resisting lateral loads in mid-rise structures. However, the arrangement of shear walls and the levels of rigid marginal beam in the building affect the structure performance. Talaeitaba et al. (2014) found that the value of response modification factor, in comparison with the presented value in ASCE7 code, was varied between -18% to +25% over changing the arrangement of the shear walls.

Earthquakes may cause extensive losses. Among which, structural damage plays an important role. One of the most important tools in evaluating the seismic damage to structures is the fragility curves. The fragility curves for certain type of building structure are used to represent the probabilities that the structural damages, under various levels of seismic excitation, exceed specified damage level. In other words, each point on the curve represents the probability that the spectral displacement under certain level of ground shaking is larger than the displacement associated with certain damage state (Cherng, 2001).

Performance-based design aims to satisfying owners and users of structures by selecting the desired performance level of the structure under different earthquakes (SEAOC, 1995; Hamburger, 1998; Federal Emergency Management Agency (FEMA) 349, FEMA/EERI, 2000; ATC, 2002; Vamvatsikos and Cornell, 2002). The desired performance level affects design and construction costs. The performance level is an expression of the maximum desired extent of damage to a structure under specific earthquake design level.

The overall building performance is categorized by FEMA 273 (1997) / 356 (2000) in terms of both the structural and non-structural performance levels as Operational, Immediate Occupancy, Life Safety and Collapse Prevention.

Incremental dynamic analysis, IDA, is a parametric analysis method used to estimate structural performance under seismic loads. During IDA, The structural model is subjected to several ground motion records, each scaled to multiple levels of intensity, and thus producing response curves parameterized versus intensity levels. IDA gives a clear vision about the performance of a certain type of structures under seismic excitations with wide range of intensities (Vamvatsikos and Cornell, 2002).

Many researchers developed and used IDA curves in their research. Uriz and Mahin (2004) used IDA to study seismic performance of concentrically braced steel frames. Kircil and Polat (2006) developed IDA curves for mid-rise RC frames in Istanbul. Mander et al. (2007) developed IDA curves for bridge structures and then the IDA results were integrated into a probabilistic risk analysis procedure. Ibrahim (2009) performed IDA on typical moment-resisting frames located in Egypt. Ibrahim and El-Shami (2011) carried out IDA for four and eight-storey multistorey reinforced concrete (RC) frame buildings in Saudi Arabia. Moridani and Khodayari (2013) studied the influence of different seismic sources characteristics on the outcomes of IDA.

Farsi et al. (2015) presented a work to estimate the seismic vulnerability of existing buildings in Algeria. Rai-pure (2015) presented a study on development of fragility curves for open ground storey buildings. She used probabilistic seismic demand model (PSDM) as per power law for the generation of fragility curves. Vazur-karand Chaudhari (2016) discussed HAZUS methodology for the generation of fragility curves and the fragility curves are generated for low-rise RC building structures without considering infill walls. Rehman and Cho (2016) produced probability damage maps for four damage levels and three structure types.

The inter-storey drift ratio, i.e. the ratio of storey drift between two consecutive floors to storey height, is considered as a significant cause that leads to the damage of building structures when subjected to earthquake ground motion. Hence, performance levels are usually expressed in terms of inter-storey drift ratios i.e. storey drift divided by storey height. FEMA 356 provided typical values of inter-storey drift ratios for different structural systems for various structural performance levels. For concrete frames, the values are 1%, 2% and 4% for immediate occupancy (IO), life safety (LS) and collapse prevention (CP), levels, respectively. Based on many references

Xue et al. (2008) suggested values of maximum inter-storey drift ratio for each performance level for different structural systems. For systems rather than that with masonry shear walls, the values of maximum inter-storey drift ratios for performance levels; operational (OP), immediate occupancy (IO), damage control (DC), life safety (LS) and collapse prevention (CP) are tabulated in Table 1.

Table 1. Maximum inter-storey drift ratios for different performance levels (Xue et al. 2008).

Performance level	OP	IO	DC	LS	CP
Maximum inter-storey drift ratio	0.005	0.010	0.015	0.02	0.025

2. Structural Models

Two reinforced concrete framed structures were selected for analysis in this research.

The first structure is one bay-eight storey space frame with 3m storey height and 4m bay width. The frames are 5m apart. Dimensions of this structure were selected so that it has a strong direction and a weak direction. In the analysis, the structure was subjected to earthquakes in the strong direction as CASE 1-1 and in the weak direction as CASE 1-2. To understand the behavior of the structure in the two studied cases, all shear walls were arranged to resist the ground motion in each case. So, four different structural systems were studied for each case. The investigated structures are described according to arrangement of shear walls as follows:

CASE 1-1
SW1: Frame without shear walls,
SW2: Frame with exterior shear walls,
SW3: Frame with interior shear walls, and
SW4: Frame with exterior and interior shear walls

CASE 1-2
SW5: Frame without shear walls,
SW6: Frame with exterior shear walls,
SW7: Frame with interior shear walls, and
SW8: Frame with exterior and interior shear walls

The second structure is a symmetric two bays-six storey space frame with 3m storey height, 4m bay width and frames are 4m apart. Six different structural systems were studied for this frame as CASE 2-0 depending on the level of the rigid marginal beam in the structure.

CASE 2-0
MB1: Structure without rigid marginal beam,
MB2: 1st storey with rigid marginal beam,
MB3: Lower storey with rigid marginal beam,
MB4: Medium storey with rigid marginal beam,
MB5: Upper storey with rigid marginal beam, and
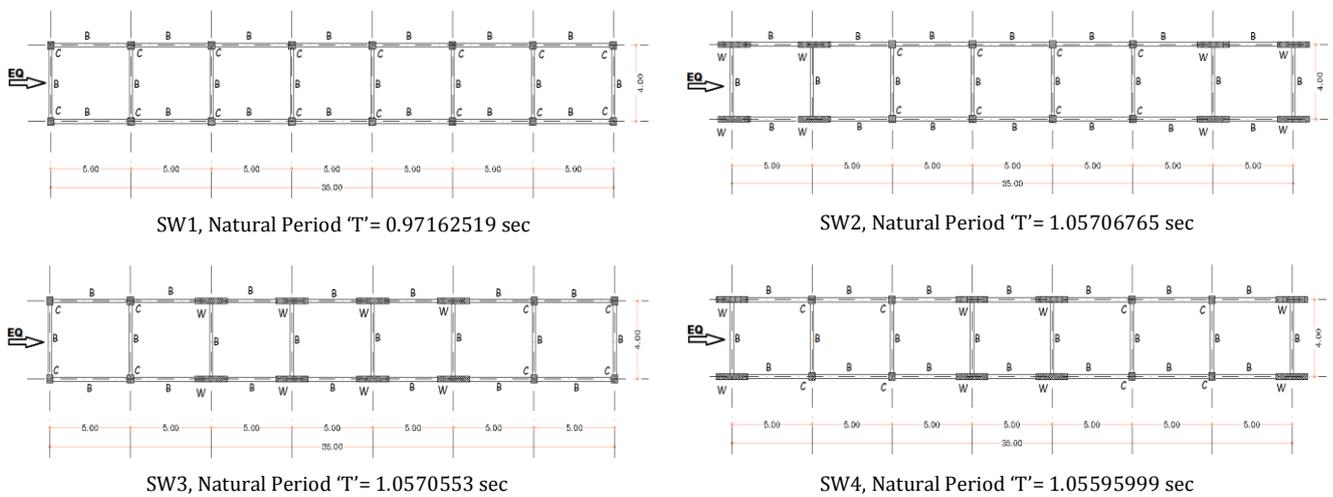MB6: All floors with rigid marginal beams.

The structure models are shown in Figs. 1, 2 and 3, while Table 2 shows the cross sections and reinforcement of beams, columns and shear walls.

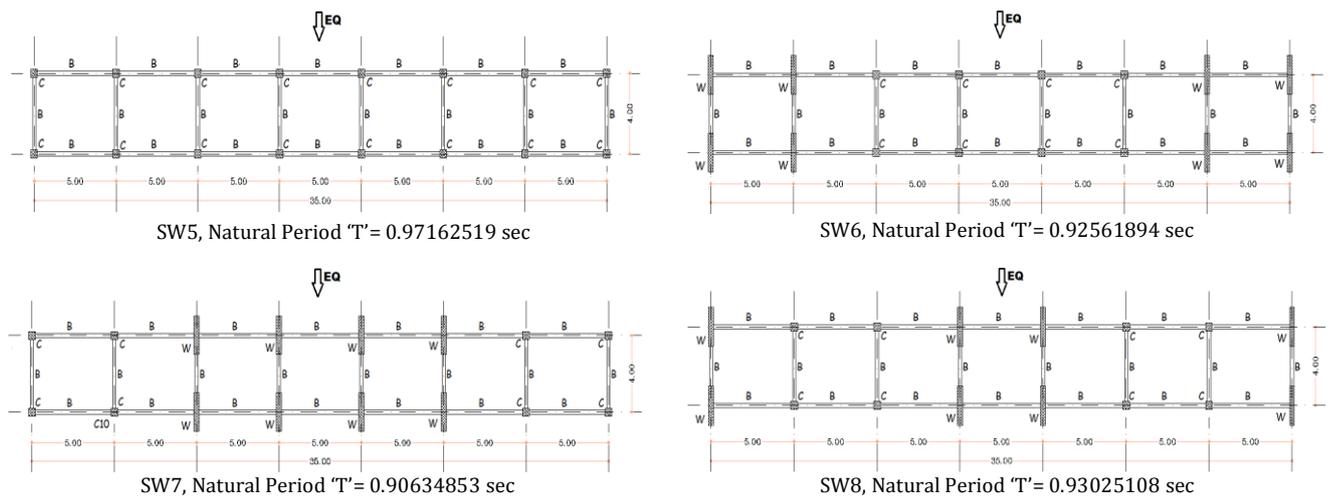All structures were designed according to the Egyptian Code of practice (No. 203, 2007) with compressive strength of concrete 250 kg/cm^2 and yielding stress of reinforcing steel 3600 kg/cm2. The soil condition was selected as soil class C, which is medium soil. The structures were classified as low hazard buildings, with importance factor I = 1. Design ground acceleration of 0.125g was considered as the structures were assumed to be in Alexandria (Zone 2).

Table 2. Cross sections of beams, columns and walls.

Model	Beam			Column	Wall
Maximum inter-storey drift ratio	B	B1	B2	C	W
Dimensions, cm	20×60	20×50	20×70	40×40	30×200
Reinforcement, mm	12Φ16	8Φ16	12Φ16	16Φ12	50Φ12

SW1, Natural Period 'T'= 0.97162519 sec

SW2, Natural Period 'T'= 1.05706765 sec

SW3, Natural Period 'T'= 1.0570553 sec

SW4, Natural Period 'T'= 1.05595999 sec

Fig. 1. Structural models for CASE 1-1 (plan views).

SW5, Natural Period 'T'= 0.97162519 sec

SW6, Natural Period 'T'= 0.92561894 sec

SW7, Natural Period 'T'= 0.90634853 sec

SW8, Natural Period 'T'= 0.93025108 sec

Fig. 2. Structural models for CASE 1-2 (plan views).

During the IDA using SeismoStruct, the concrete was modeled using a uniaxial constant confinement concrete model initially presented by Madas (1993). The confinement effects provided by the lateral transverse reinforcement are included through the model introduced by Mander et al. (1988) which assumed constant confining pressure throughout the entire stress–strain range. The reinforcing bars were modeled using a uniaxial bilinear stress-strain model with kinematic strain hardening.

The elastic range remains constant throughout the various loading stages, and the kinematic hardening rule for the yield surface is assumed as a linear function of the increment of plastic strain.
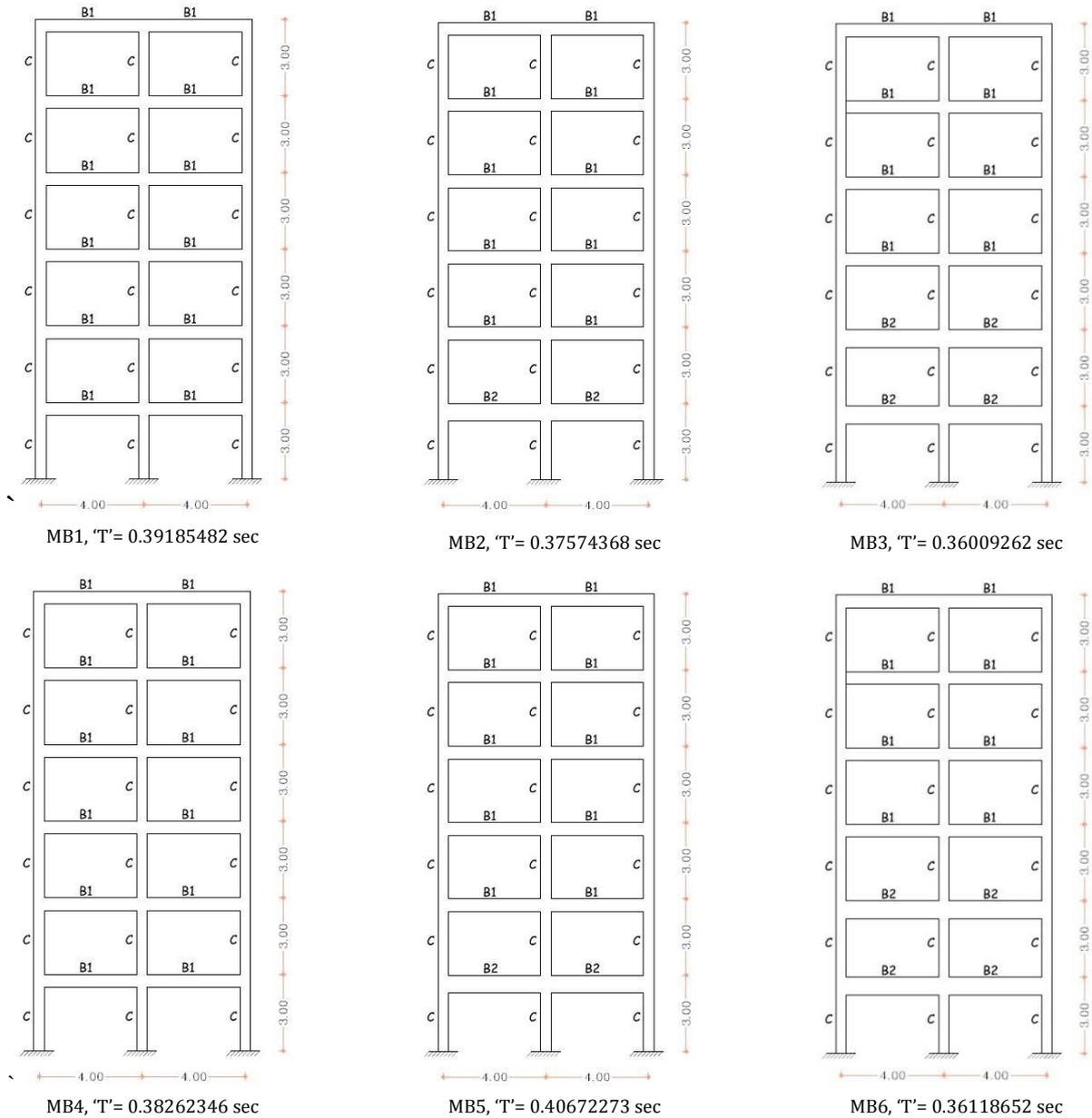
MB1, 'T'= 0.39185482 sec

MB2, 'T'= 0.37574368 sec

MB3, 'T'= 0.36009262 sec

MB4, 'T'= 0.38262346 sec

MB5, 'T'= 0.40672273 sec

MB6, 'T'= 0.36118652 sec

Fig. 3. Structural models for CASE 2-0 (elevation views)

3. Incremental Dynamic Analysis

To perform IDA, an appropriate set of ground motions is required. Several seismic codes (e.g. Uniform Building Code (UBC), 1997; Egyptian code for loads and ENV 1998-1, 2005) and researchers (e.g. Bommer et al., 2003) suggested a minimum of seven ground motions to be used to describe the behavior of a building under seismic loads. These ground motions can be selected from real records of earthquakes or can be generated artificially. Real records are more realistic since they include all ground motions characteristics such as amplitude, frequency, duration, energy content, number of cycles and phase (Rota et al., 2010). In this analysis, 10 records of ground motions were selected to perform the time history analysis of the chosen structures; all of them are real records of historical earthquakes. The characteristics of these ground motions are presented in Table 3.

During IDA, each ground motion was scaled incrementally up to 1.0g using a step of 0.2g. The maximum inter-storey drift ratio was calculated for each PGA, this represents a point on the IDA curve. The points of this drift ratio resulting from the various PGA values form the full IDA curve for a specific ground motion. The procedure was repeated for all 10 ground motions used in this paper. The full of fourteen IDA curves was extracted. Each curve characterizes the seismic response of a specific structural model under the effect of the ten ground motions. The IDA curves for the structural models are presented in Figs 4, 5 and 6 for CASE 1-1, CASE 1-2 and CASE 2-0 respectively.

The number of occurrence among the ground motions that exceeded certain performance level at each PGA value is calculated. Then the probability of exceeding this damage state was calculated. Mean and standard deviation, μ and σ, of the natural logarithm of PGA at

which each structure reaches the threshold of a specific damage state or performance level were calculated. These values are summered in Tables 4, 5 and 6 for CASE 1-1, CASE 1-2 and CASE 2-0 respectively, and were used in developing the fragility curves presented below.

As can be noted from all curves, IDA curve differs from one ground motion to another leading to a wide range of response for each structure. The common property shared by all curves is that data points create a linear region at lower scale factors. By increasing scale factor the curves begin to bend meaning that the structure begins to yield. For better assessment of structural performance, seismic fragility curves for each structure needs to be extracted at the five performance levels tabulated in Table 1.

The vertical gridlines on each curve at maximum inter-storey drift ratio of 0.005, 0.01, 0.015, 0.02 and 0.025 represent performance level of OP, IO, DC, LS and CP respectively.

Table 3. Details of ground motions

No.	Ground motion	Station	Date	PGA (g)	Duration, Sec.
1	CHICHI	TAIWAN	Sep,20,1999	0.36	50
2	FRIULI	ITALY	May,06,1976	0.35	36
3	HOLLISTER	USA	Apr,09,1961	0.2	40
4	IMPERIAL VALLEY	USA	Oct,15,1979	0.32	40
5	KOBE	JAPAN	Jan,16,1995	0.34	40
6	KOCAELI	TURKEY	Aug,17,1999	0.35	35
7	LANDERS	USA	Jun,28,1992	0.64	48
8	LOMA, PRIETTA	USA	Oct,18,1989	0.36	40
9	NORTHRIDGE	USA	Jan,17,1994	0.57	40
10	TRNIDAD	USA	Aug,24,1983	0.19	21

4. Fragility Curves

Fragility curves are log-normal functions which express the probability of reaching or exceeding a specific damage state. They can be developed in terms of a seismic parameter, such as spectral acceleration, spectral displacement, peak ground velocity and PGA. Since PGA was the parameter used in developing the IDA in this work and also in previous researchers such as Ibrahim and El-Shami (2010), the PGA was selected to be the corresponding parameter in developing the fragility curves. The cumulative distribution functions was calculated by dividing the number of data points that reached or exceeded a particular damage state by the number of data points of the whole sample (Shinozuka et al., 2003). The conditional probability of a structure to reach or exceed a specific damage state, D, given the PGA, is defined by:

$$P\left[D/PGA\right] = \phi\left((\ln\left(PGA\right) - \mu)/\sigma)\right), \qquad (1)$$

where ϕ is the standard normal cumulative distribution function; μ and σ are the mean value and standard deviation of the natural logarithm of PGA at which the building reach the threshold of a specific damage state or performance level; D. Log-normal functions with two parameters (μ and σ) were fitted for different performance levels: OP, IO, DC, LS and CP, associated with the frames under study.

The input data points and the log-normal function fitted for different performance levels occurred in frame [SW1] (as an example) are shown in Table 7 and Fig. 7.

Referring to Table 7, it can be noticed that when frame SW1 is exposed to weak ground motion with PGA = 0.2g, the probabilities of exceeding the OP, IO, DC, LS and CP performance levels are 69%, 36%, 5%, 4% and 1% respectively. Also, the probability of exceeding a certain performance level increases by increasing PGA. Relations between PGA and probability for different performance levels of frame SW1 are plotted in Fig. 7 whereas Figs. 8, 9 and 10 represent the whole set of fragility curves for frames of CASE 1-1, CASE 1-2 and CASE 2-0 respectively.

It is obvious that in CASE 1-1, the probability of exceeding different performance levels for frame (SW1) is higher than its counterpart in (SW2) with a significant difference. This indicates that existence of exterior shear walls significantly enhances performance of the structure at different levels.

Interior shear walls (SW3) show slight improvement in performance of the structure compared to exterior shear walls (SW2).

Distributing shear walls externally and internally (SW4) gives an intermediate response between those for SW2 and SW3.

Generally, it is clear that different arrangements of shear walls along the strong direction of the structure have little effects on structural performance but the best performance was achieved when shear walls were accumulated internally. On the other hand, when earthquakes act on the weak direction of the structure (CASE 1-2), existence of exterior shear walls (SW6) slightly improves performance when compared to (SW5).
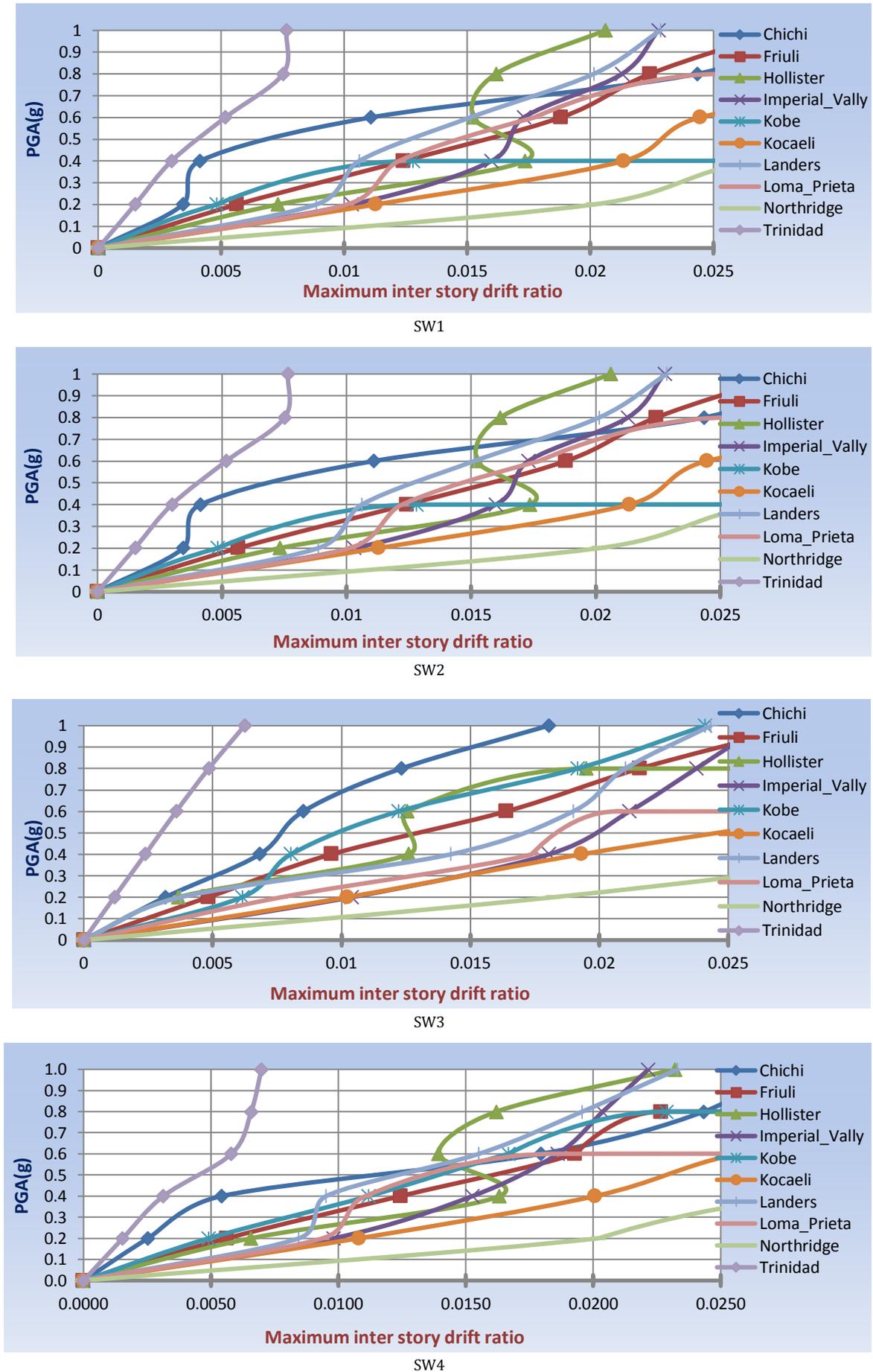
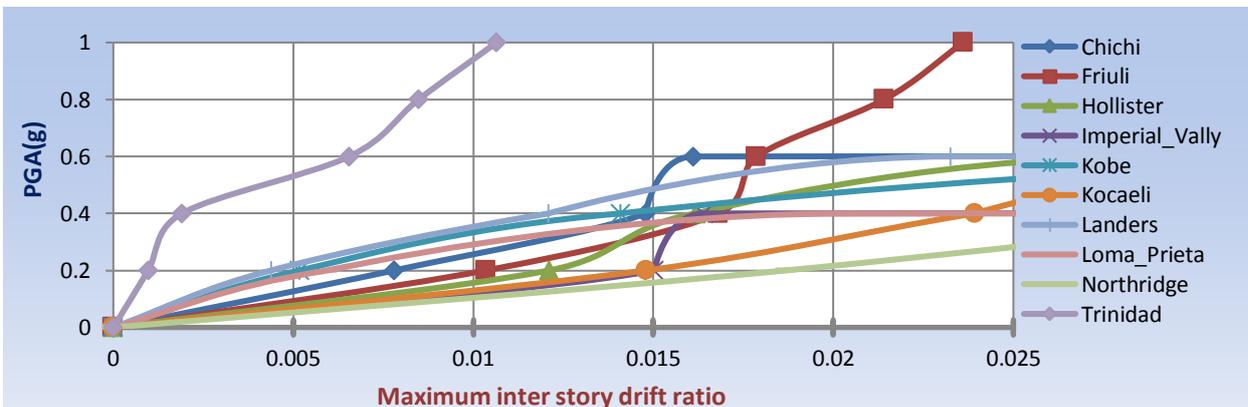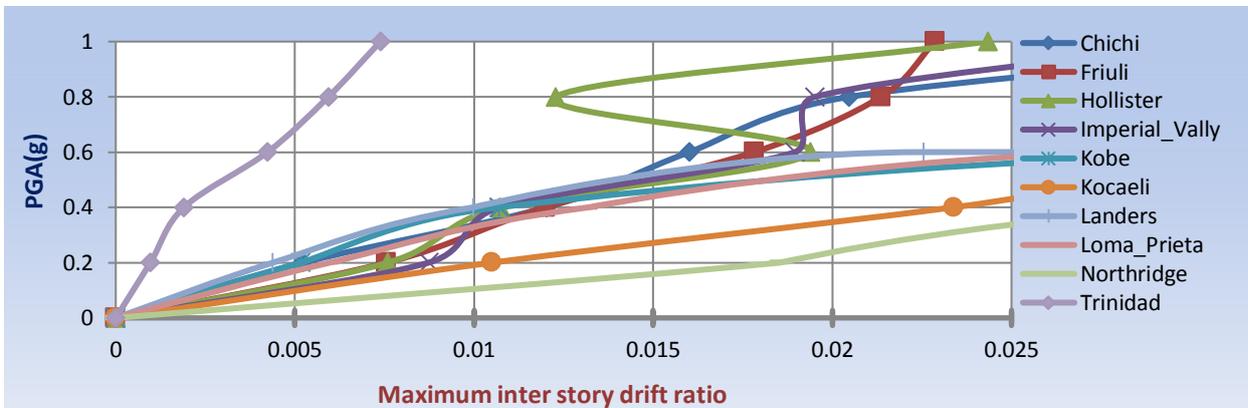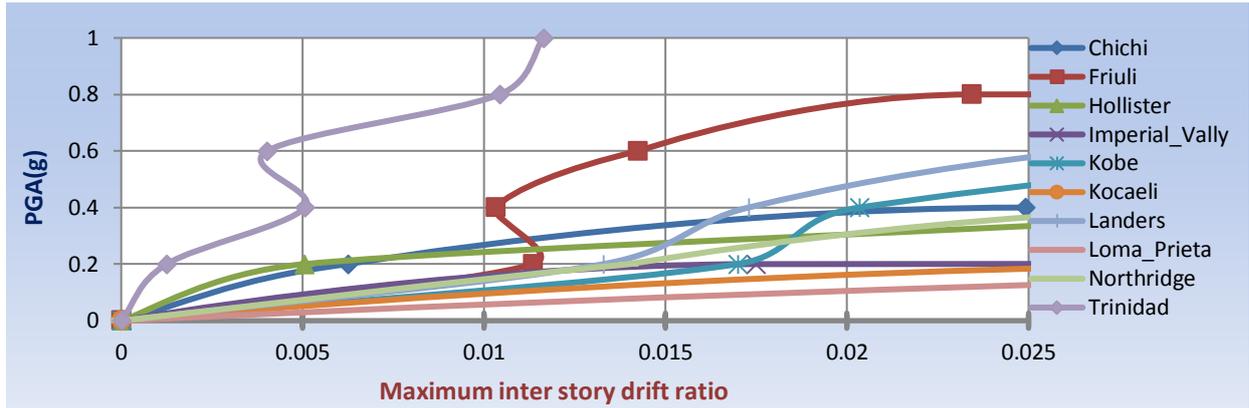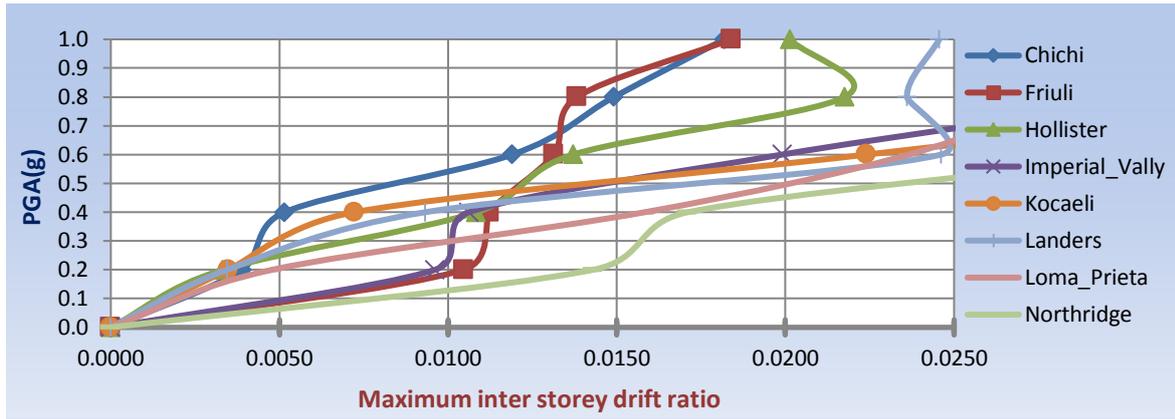**Fig. 4.** Incremental dynamic analysis for the four frames in CASE 1-1.
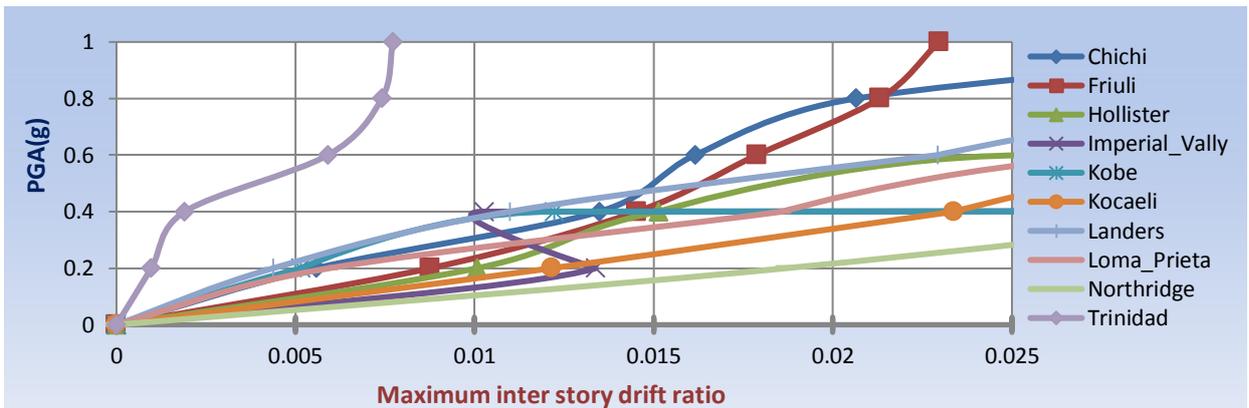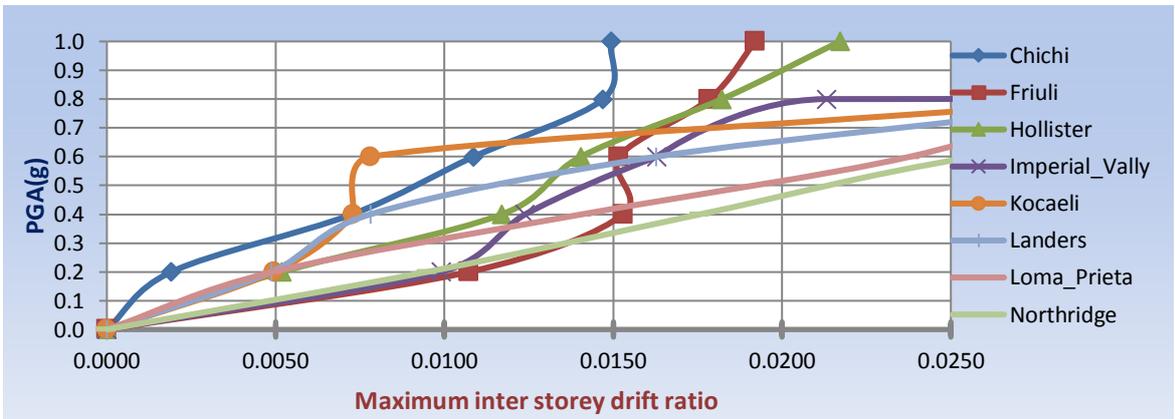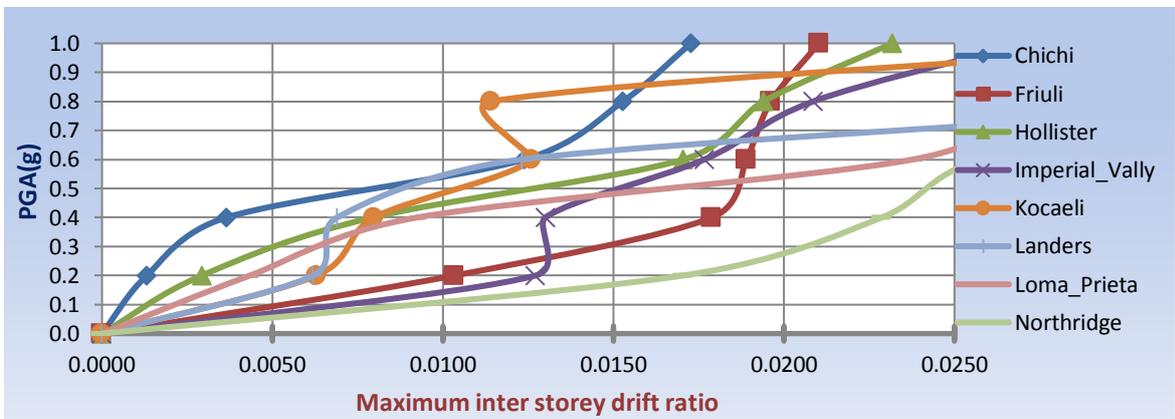
Fig. 5. Incremental dynamic analysis for the four frames in CASE 1-2.
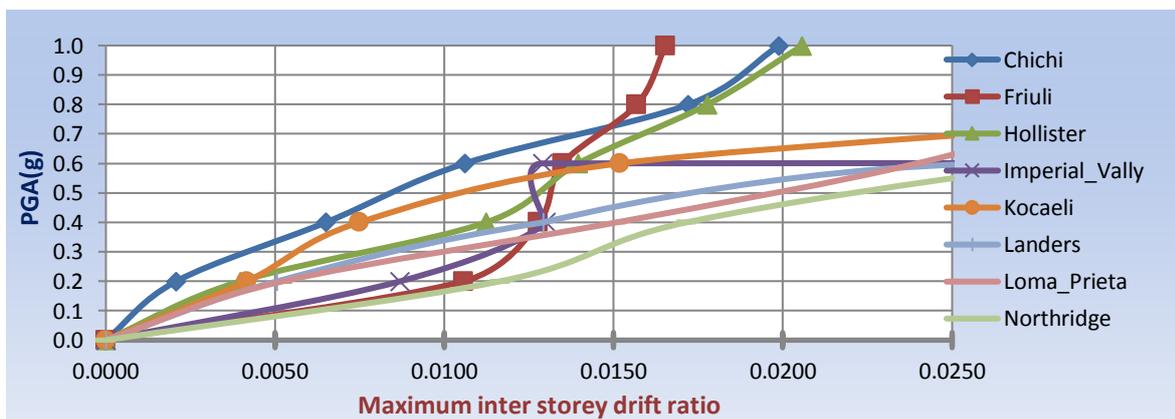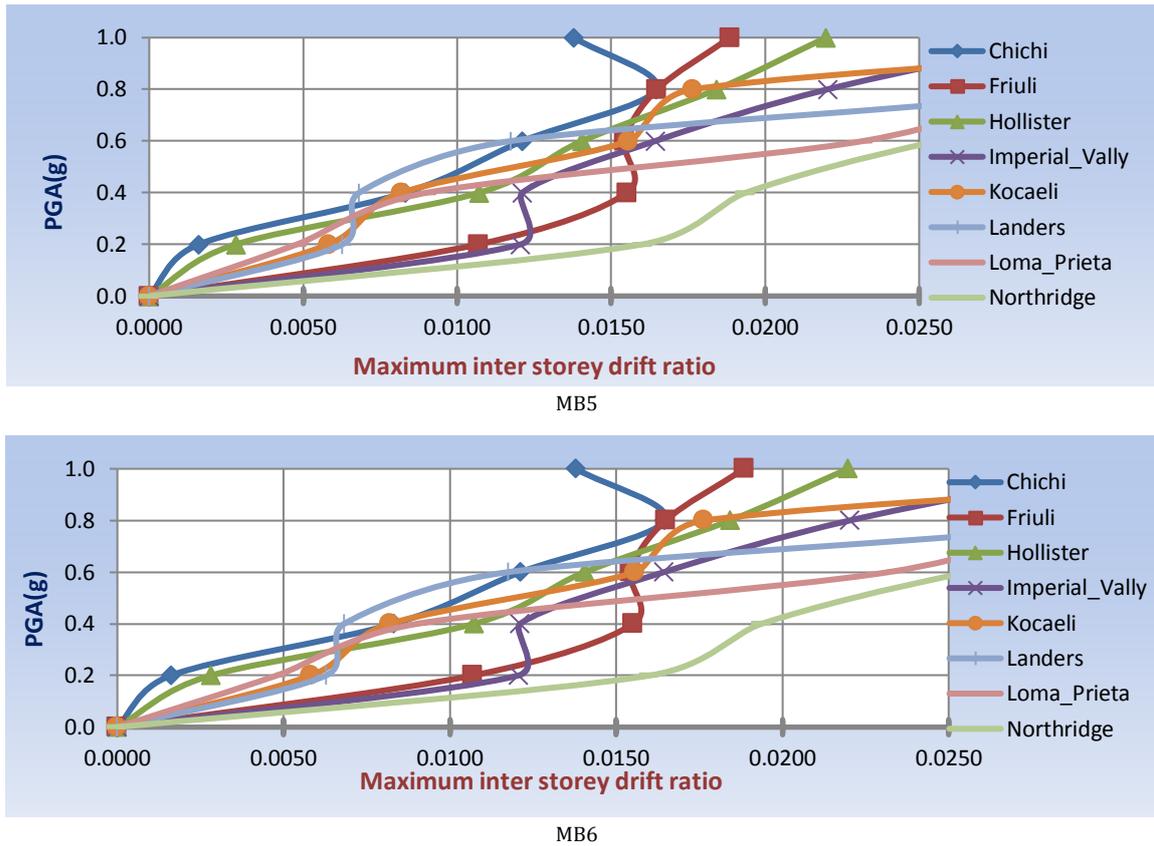
MB1

MB2

MB3

MB4

MB5

MB6

Fig. 6. Incremental dynamic analysis for the six frames in CASE 2-0.

Table 4. Parameters of log-normal distributions for fitting data for CASE 1-1 frames.

Frames	OP		IO		DC		LS		CP	
	μ	σ	μ	σ	μ	σ	μ	σ	μ	σ
SW1	0.128	0.925	0.259	0.726	0.438	0.477	0.494	0.505	0.596	0.470
SW2	0.108	0.900	0.237	0.878	0.410	0.535	0.562	0.567	0.825	0.580
SW3	0.150	0.855	0.297	0.801	0.447	0.630	0.628	0.628	0.914	0.656
SW4	0.108	0.900	0.273	0.786	0.430	0.513	0.637	0.578	0.896	0.544

Table 5. Parameters of log-normal distributions for fitting data for CASE 1-2 frames.

Frames	OP		IO		DC		LS		CP	
	μ	σ	μ	σ	μ	σ	μ	σ	μ	σ
SW5	0.069	0.824	0.142	0.786	0.212	0.943	0.286	0.821	0.309	0.861
SW6	0.119	0.789	0.223	0.860	0.370	0.613	0.455	0.547	0.550	0.467
SW7	0.223	0.549	0.270	0.748	0.431	0.511	0.594	0.449	0.714	0.517
SW8	0.093	0.909	0.209	0.902	0.337	0.651	0.437	0.541	0.529	0.500

Table 6. Parameters of log-normal distributions for fitting data for CASE 2-0 frames.

Frames	OP		IO		DC		LS		CP	
	μ	σ	μ	σ	μ	σ	μ	σ	μ	σ
MB1	0.146	0.579	0.234	0.522	0.443	0.420	0.610	0.441	0.734	0.417
MB2	0.116	0.416	0.294	0.525	0.493	0.275	0.726	0.359	0.818	0.289
MB3	0.137	0.582	0.277	0.599	0.438	0.454	0.693	0.482	0.842	0.334
MB4	0.123	0.477	0.287	0.398	0.486	0.282	0.668	0.382	0.734	0.417
MB5	0.137	0.582	0.278	0.383	0.423	0.374	0.578	0.439	0.684	0.490
MB6	0.123	0.477	0.260	0.567	0.445	0.373	0.728	0.428	0.842	0.334

Table 7. The probability of exceeding performance levels at certain PGA for frame [SW1].

PGA(g)	OP	IO	DC	LS	CP
0.0	0.00	0.00	0.00	0.00	0.00
0.1	0.39	0.09	0.00	0.00	0.00
0.2	0.69	0.36	0.05	0.04	0.01
0.3	0.82	0.58	0.21	0.16	0.07
0.4	0.89	0.72	0.42	0.34	0.20
0.5	0.93	0.82	0.61	0.51	0.35
0.6	0.95	0.88	0.74	0.65	0.51
0.7	0.97	0.91	0.84	0.76	0.63
0.8	0.98	0.94	0.90	0.83	0.73
0.9	0.98	0.96	0.93	0.88	0.81
1.0	0.99	0.97	0.96	0.92	0.86

The probability of exceeding the performance levels for frame (SW7) is lower than its counterpart in (SW6), this clarifies that existence of interior walls provides the structure with more efficiency than of exterior walls. In (SW8), the same number of walls was used but was distributed externally and internally. It was observed that the probability of reaching different performance levels in this case is higher than (SW7) and lower than (SW6). Based on the previously discussed results, it can be concluded that the best performance of the structure was reached in case of interior shear walls.

It is obvious that in CASE 2-0, the probability of exceeding the performance levels for the frame in the cases [MB1], [MB4] and [MB5] are higher than their counterparts in the case [MB2], [MB3] and [MB6], which means that existence of rigid marginal beam in lower levels gives more efficiency.

Lateral load resisting efficiencies in structure with rigid marginal beams in all floors and that for rigid marginal beam in the 1st floor are almost the same. This indicates that the existence of rigid marginal beam in the lower storey provides the best performance and the most economic situation.
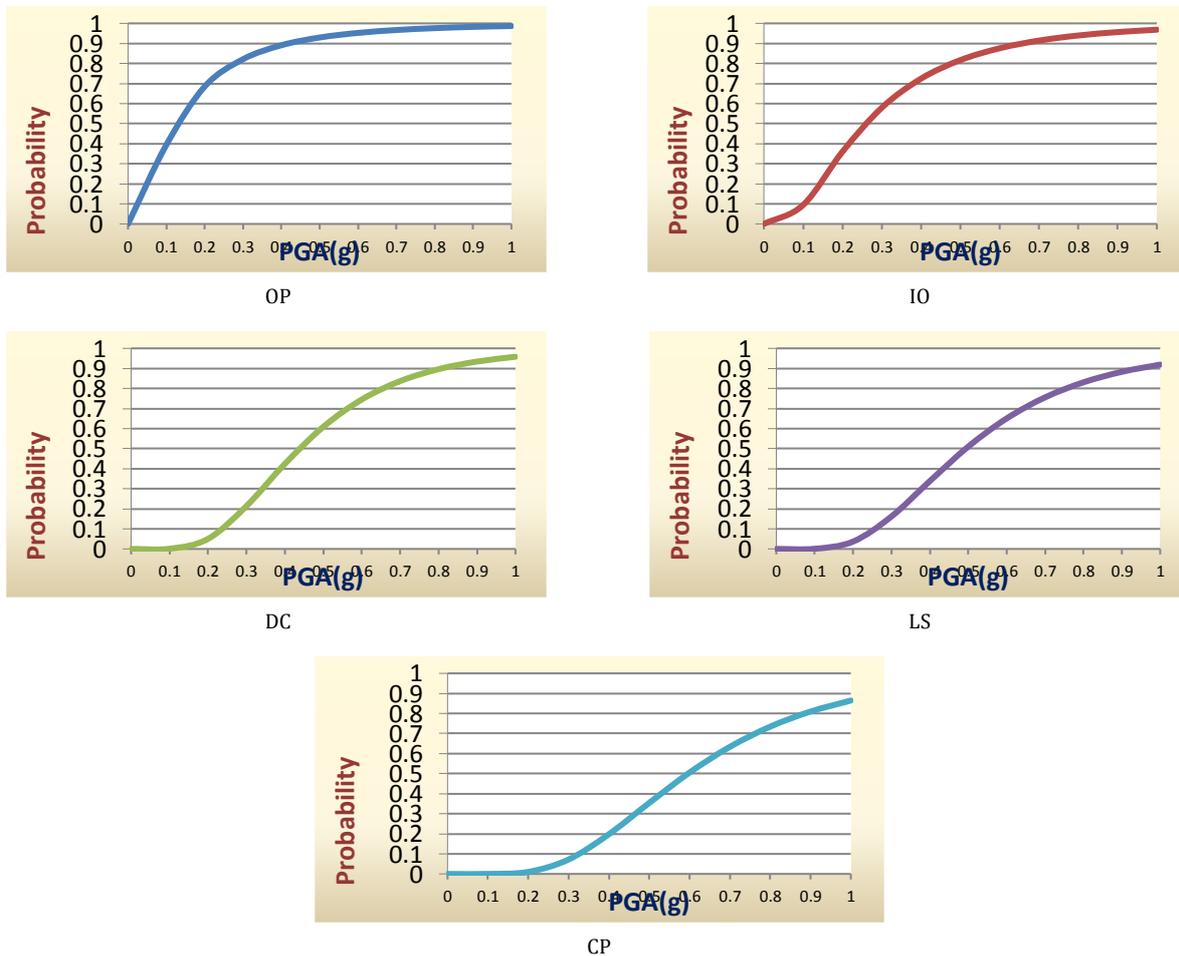
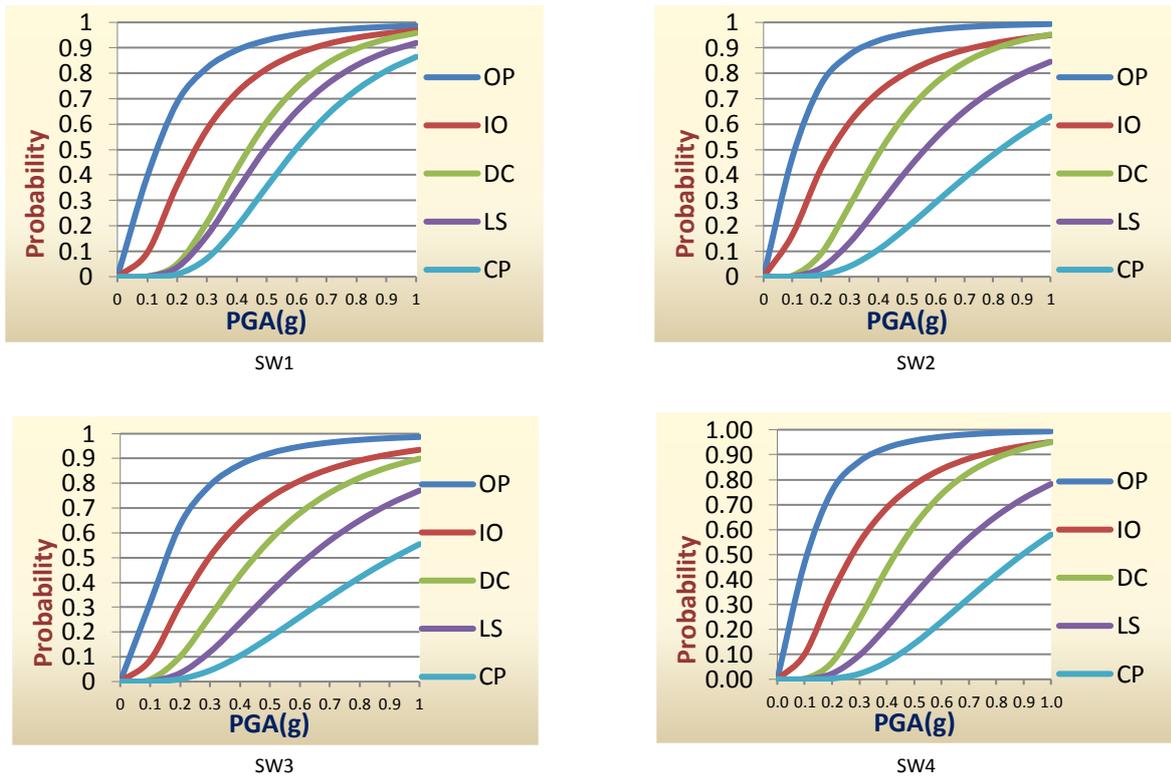**Fig. 7**. Fitted curves for the frame SW1 at different performance levels.

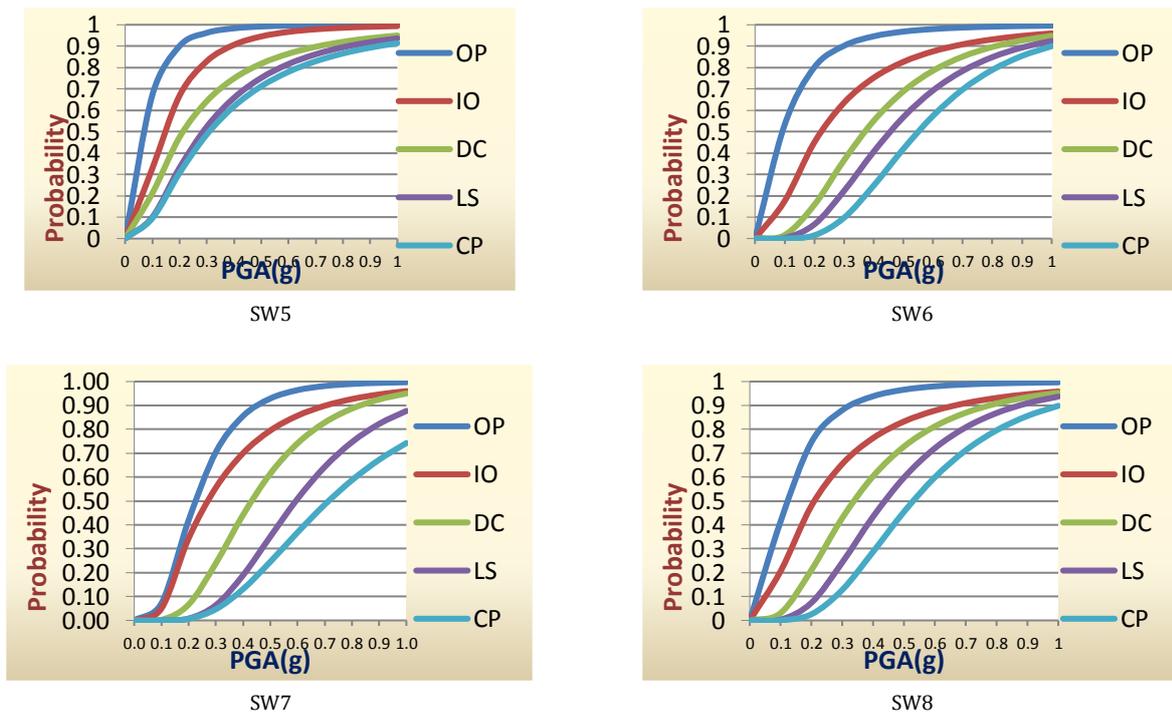**Fig. 8.** Fragility curves for frames of CASE 1-1.

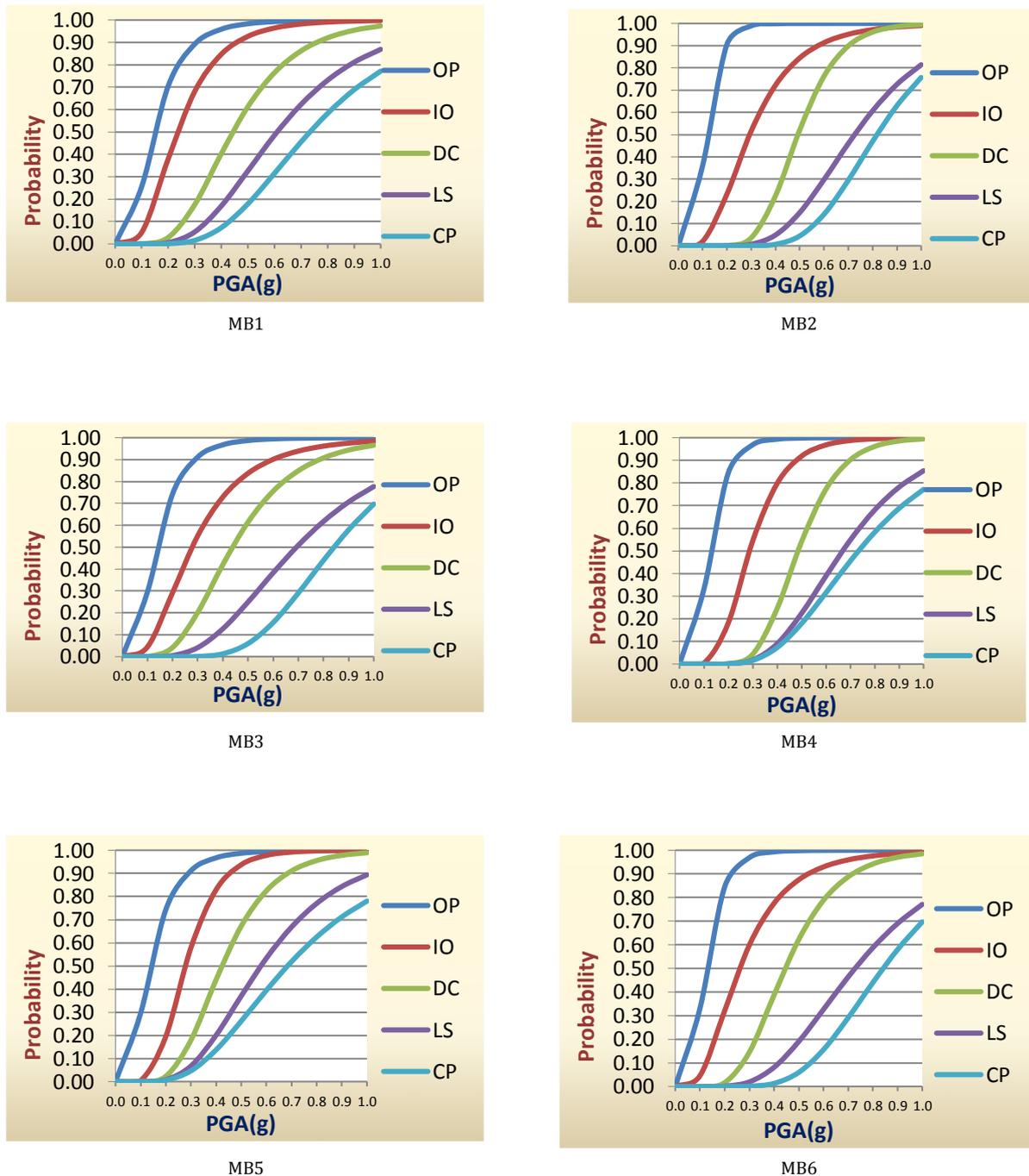**Fig. 9.** Fragility curves for frames of CASE 1-2.

Fig. 10. Fragility curves for frames of CASE 2-0.

5. Conclusions

In this study, seismic fragility curves were conducted for R.C. 3D framed structures with different positions of shear walls as the first category of cases, two cases were considered CASE 1-1 and CASE 1-2 where in CASE 1-1, the structure was exposed to ground motions in its long direction while in CASE 1-2 ground motions act in the short direction. Ground motions were obtained from real records.

Also in this study, seismic fragility curves were conducted for R.C. 3D framed structures with different levels of the rigid marginal beam.

IDA was conducted using 'SeismoStruct' software under 10 ground motions. IDA curves showed wide range of behavior with large variation from record to record.

Different structural and non-structural performance levels were considered. These levels are operational (OP), immediate occupancy (IO), damage control (DC), life safety (LS) and collapse prevention (CP).

Based on the obtained results for different studied cases, it can be concluded that:

- Fragility curves are very useful tools for describing the behavior of certain structure under seismic loads. They also are considered as an excellent means of judgment and hence predicting the most efficient system for a certain structure.

- Different arrangements of shear walls in the structure produce different responses which lead to different performances.
- In frames of CASE1-1, shear walls, generally, play an important role in improving seismic performance of the structure, but no significant differences in performance were observed regarding to wall arrangement in the structure.
- In frames of CASE1-2, using interior shear walls gives the best behavior of the structure compared to exterior shear walls only and distributing shear walls internally and externally.
- The existing of rigid marginal beam in the lower storey shows the best structural resistance for lateral loads.

REFERENCES

ATC (2002). Development of Performance-Based Earthquake Design Guidelines. Redwood City: ATC-58.

Bommer JJ, Acevedo AB, and Douglas J (2003). The selection and scaling of real earthquake accelerograms for use in seismic design and assessment. In: Proceeding of ACI international conference on seismic bridge design and retrofit. La Jolla, CA: American Concrete Institute.

Cherng R (2001). Preliminary Study on the Fragility Curves for Steel Structures in Taipei. *Earthquake Engineering and Engineering Seismology*, 3(1), 35-42.

ECP 203 (2007). Egyptian code of practice for design and construction of concrete structures. National Center of Housing and Building Researches, Cairo, Egypt.

ENV 1998-1 (2005). Eurocode8: Design of Structures for Earthquake Resistance – Part 1: General rules, seismic actions and rules for buildings, Code of Practice, London.

Farsi M, Cherif F, Kaci S, Belaidi O, Taouche-Kheloui F (2015). Seismic vulnerability of reinforced concrete structures in Tizi-Ouzou City (Algeria). *1st International Conference on Structural Integrity,* 2015, 838-845.

Federal Emergency Management Agency (FEMA) 273 (1997). NEHRP guidelines for the seismic rehabilitation of buildings. Washington DC: Federal Emergency Management Agency.

Federal Emergency Management Agency (FEMA) 349, FEMA/EERI (2000). Action plan for performance – based seismic design. Washington DC: Federal Emergency Management Agency.

Federal Emergency Management Agency (FEMA) 356 (2000). Prestandard and commentary for the seismic rehabilitation of buildings. Washington DC: Federal Emergency Management Agency.

Federal Emergency Management Agency (FEMA) 450 (2003). NEHRP recommended provisions for seismic regulations for new buildings and other structures, Part 1: provisions. Washington DC: Federal Emergency Management Agency.

Hamburger RO (1998). Performance-based analysis and design procedure for moment resisting steel frames. Background Document, SAC Steel Project.

Heidebrecht A (2004). Code development issues arising from the preparation of the seismic provisions of the national building Code of Canada. 13WCEE, Vancouver, Canada: 3218-3228.

Ibrahim Y (2009). Performance limits of mid-rise moment-resisting framed structures in low seismicity areas. *11th Arab Structural Engineering Conference*, 25-27 October. Dhahran, Saudi Arabia: KFUPM.

Ibrahim Y and El-Shami M (2011). Seismic fragility curves for mid-rise reinforced concrete frames in Kingdom of Saudi Arabia. The IES Journal Part A: Civil & Structural Engineering, 4(4), 213-223

International Building Code (IBC) (2003). CA, USA: International Code Council, Delmar Cengage Learning.

Japan Structural Consultants Association (JSCA) (2000). Structural Design by Response Control Methods. Shoko-kusha Publishing Co. Ltd., Tokyo, Japan [in Japanese].

Khawar R, Yong-Sik C (2016). Building Damage Assessment Using Scenario Based Tsunami Numerical Analysis and Fragility Curves. Department of Civil and Environmental Engineering, Hanyang University, 222 Wangsimni-ro, Seongdong-gu, Seoul 04763, Korea; (CC-BY) license (http://creativecommons.org/licenses/by/4.0/).

King A, Shelton R (2004). New Zealand advances in performance-based seismic design. *13WCEE*, Vancouver, Canada: 13–25.

Kircil M, Polat Z (2006). Fragility analysis of mid-rise R/C frame buildings. *Engineering Structures*, 28(9), 1335-1345

Madas P (1993). Advanced Modeling of Composite Frames Subjected to Earthquake Loading. *Ph.D. Thesis,* London, UK: Imperial College, University of London.

Mander J, Dhakal R, Mashiko N, Solberg K (2007). Incremental dynamic analysis applied to seismic financial risk assessment of bridges. *Engineering Structures,* 29(10), 2662-2672.

Mander J, Priestley M, Park R (1988). Theoretical stress-strain model for confined concrete. *Journal of Structural Engineering,* 114(8), 1804-1826.

Moridani K, Khodayari R (2013). Seismic performance assessment uses incremental dynamic analysis. *Journal of Basic and Applied Scientific Research*, 3(8), 757-764.

Raipure P (2015). Seismic vulnerability assessment of open ground storey RC buildings by using fragility curves. *M-Tech Thesis*, Government College of Engineering, Amravati, 2013-14.

Rota M, Penna A, Magnes G (2010). A methodology for deriving analytical fragility curves for masonry buildings based on stochastic nonlinear analyses. Engineering Structures, 32, 1312-1323.

SeismoStruct Ver. 5.0.4, 2010. SeismoSoft, earthquake engineering software solutions [online]. Italy. Available from: www.seismosoft.com [Accessed 10 August 2011].

Shome N, Cornell CA (1999). Probabilistic Seismic Demand Analysis of Nonlinear Structures. *Ph.D. Thesis,* Stanford: Stanford University.

Structural Engineers Association of California, SEAOC, Vision 2000 (1995). Performance based seismic engineering of buildings. Sacramento, CA: Vision 2000 Committee.

Talaeitaba S, Tahvilian H, Saeedi B (2014). The effect of the arrangement and length of the concrete shear walls on the response modification factor (R). *Electronic Journal of Structural Engineering,* 14, 93-105.

Uriz P, Mahin S (2004). Seismic performance assessment of concentrically braced steel frames. *13th World Conference on Earthquake Engineering*, Vancouver, B.C., Canada

Vamvatsikos D, Cornell C.A (2002). Incremental dynamic analysis. *Journal of Earthquake Engineering and Structural Dynamics,* 31(3), 491-514.

Vazurkar U, Chaudhari D (2016). Development of fragility curves for RC buildings. *International Journal of Engineering Research,* 5(3), 591-594.

Xue Q, Wu CW, Chen CC, Chen KC (2008). The draft code for performance-based seismic design of buildings in Taiwan. *Engineering Structures*, 30(6), 1535–1547.